GSI

GSI-Preprint-96-38
August 1996

PRESENT STATUS AND FUTURE ASPECTS OF NUCLEAR STRUCTURE CLOSE TO ^{100}Sn

H. GRAWE, M. GORSKA, M. LIPOGLAVSEK, R. SCHUBART, A. ATAC, A. AXELSSON, J. BLOMQVIST, J. CEDERKÄLL, G. de ANGELIS, M. de POLI, C. FAHLANDER, A. JOHNSON, K.H. MAIER, L.-O. NORLIN, J. NYBERG, D. FOLTESCU, M. PALACZ, J. PERSSON, M. REJMUND, H.A. ROTH, T. SHIZUMA, Ö. SKEPPSTEDT, G. SLETTEN, M. WEISZFLOG, AND THE OSIRIS, NORDBALL-PEX AND EUROBALL COLLABORATIONS

(Invited contribution, International Conference on Nuclear Structure at the Turn of the Century, Crete, Greece, 1.- 6.7.1996, to be published in Z. Phys. A)

Gesellschaft für Schwerionenforschung mbH
Planckstraße1 • D-64291 Darmstadt • Germany
Postfach 110552 • D-64220 Darmstadt • Germany

Noname Manuscript-Nr.
(will be inserted by hand later)

Present Status and future aspects of nuclear structure close to ^{100}Sn

H. Grawe[1,2], M. Gorska[1,2,3], M. Lipoglavsek[4,5], R. Schubart[1], A. Atac[5], A. Axelsson[6], J. Blomqvist[6], J. Cederkäll[6], G. de Angelis[7], M. de Poli[7], C. Fahlander[5,7], A. Johnson[6], K.H. Maier[2], L.-O. Norlin[6], J. Nyberg[5], D. Foltescu[8], M. Palacz[10], J. Persson[5], M. Rejmund[1,2,3], H.A. Roth[8], T. Shizuma[9], O. Skeppstedt[8], G. Sletten[9], M. Weiszflog[5], and the OSIRIS, NORDBALL-PEX and EUROBALL collaborations

[1] Gesellschaft für Schwerionenforschung, P.O. Box 110552, D-64220 Darmstadt, Germany
[2] Hahn-Meitner-Institut, P.O. Box 390128, D-14091 Berlin, Germany
[3] Institute of Experimental Physics Warsaw University, Warsaw, Poland
[4] J. Stefan Institute, Ljubljana, Slovenia
[5] The Svedberg Laboratory, Uppsala University, Uppsala, Sweden
[6] Department of Physics, Royal Institute of Technology, Stockholm, Sweden
[7] INFN, Laboratori Nazionali di Legnaro (Padova), Italy
[8] Chalmers University of Technology, Gothenburg, Sweden
[9] Niels Bohr Institute, University of Copenhagen, Denmark
[10] Soltan Institute for Nuclear Studies, Swierk, Poland

Received 6 August 1996

Abstract. The present status of experimental approach to ^{100}Sn in the spectroscopy of excited states is landmarked by the T_z=3/2 nuclei between ^{95}Pd and ^{101}In and the T_z=1 nuclei ^{94}Pd and ^{98}Cd. The detection limits with Pre-EUROBALL γ-arrays and ancillary detectors are below the 10^{-5} level of the total fusion- evaporation residue cross section. A large scale shell model analysis of the existing data reveals the shell structure at ^{100}Sn, which shows a remarkable similarity to ^{56}Ni. Evidence for an increasing proton-neutron interaction in approaching the N=Z line is deduced from high spin isomers and spherical yrast lines. The effective E2 operator for protons and neutrons and implications for a low lying particle-hole (ph) E2 excitation in ^{100}Sn are discussed.

PACS: 21.10.sf, 21.60.Cs, 23.20.-g, 27.60.+j

1 Introduction

The doubly magic nucleus ^{100}Sn has attracted much attention in the past in β^+/EC [1] and in-beam experiments [2] following heavy ion fusion-evaporation reactions, and in fragmentation of high energy heavy ion beams [3, 4]. Nevertheless the nuclear structure information on ^{100}Sn and its one- and two-particle (hole) neighbours is scarce and its shell structure has to be deduced from excited states in more remote nuclei, which are accessible to exclusive β^+/EC and in-beam studies. This review is therefore restricted to the shell model analysis of these nuclei with the main emphasis on recent in-beam experiments. In Fig. 1 the present status of experimental approach to ^{100}Sn in these experiments is shown, with the boarderline of detection marked by the T_z=1 nuclei ^{94}Pd [5], ^{98}Cd [6], the T_z=3/2 ^{95}Pd [7], ^{97}Ag [8], ^{99}Cd [9], and ^{101}In [10], and the T_z=2 nuclei between ^{96}Pd and ^{106}Sb as reviewed in a recent article [2]. The experimental data were obtained at the OSIRIS (HMI Berlin), NORDBALL and NORDBALL-PEX arrays (NBI Roskilde).

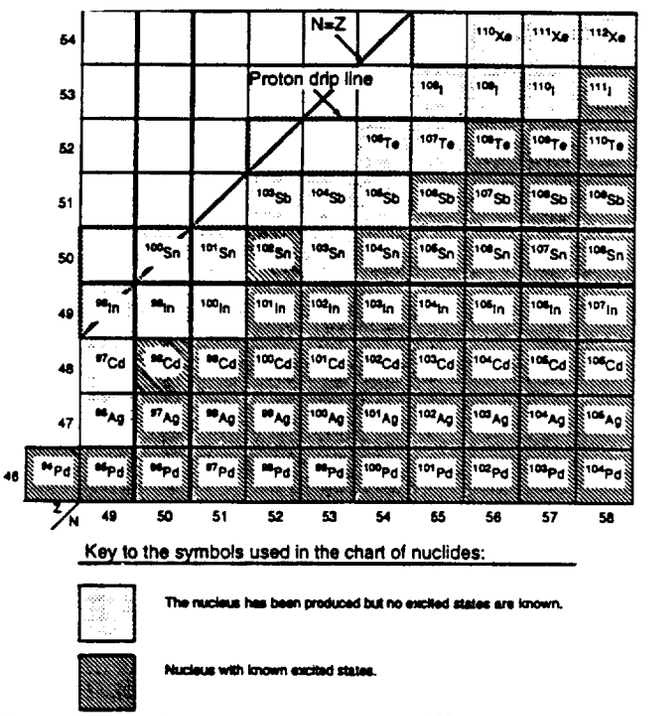

Fig. 1. Status of experimental approach to ^{100}Sn. The N=Z line and the proton dipline are indicated. The relevant shell model orbits are $p_{1/2}$, $g_{9/2}$ below the N=Z=50 shell closure and $d_{5/2}$, $g_{7/2}$, $s_{1/2}$, $d_{3/2}$ and $h_{11/2}$ above ^{100}Sn both for protons and neutrons.

2 The experimental approach to ^{100}Sn

The in-beam spectroscopy of neutron deficient nuclei below the 1 % level of the total fusion-evaporation residue cross section requires a highly selective setup including a powerful γ-array and efficient ancillary detectors for

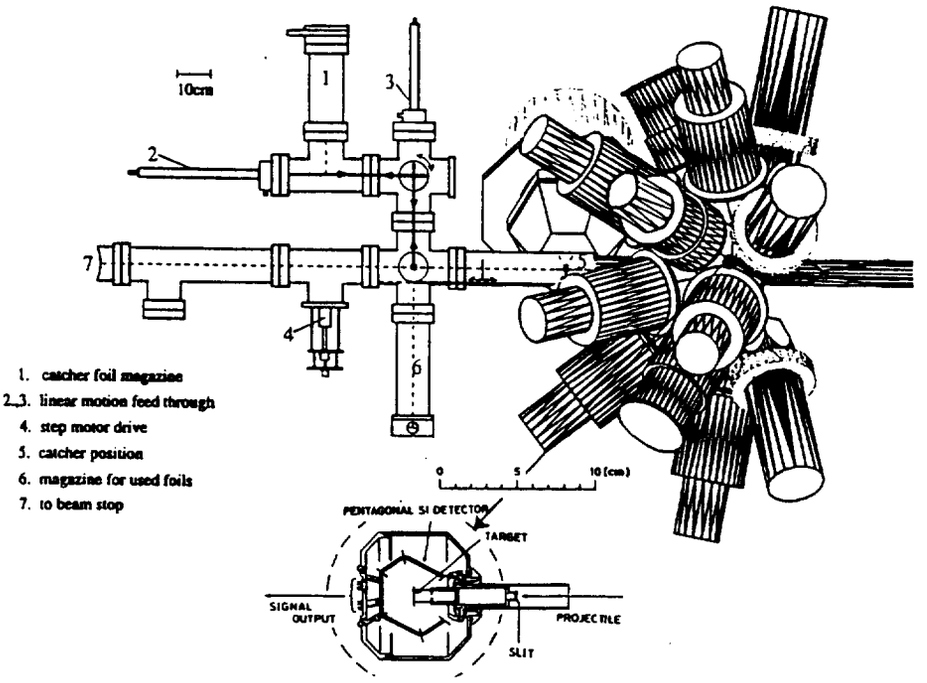

Fig. 2. NORDBALL–PEX array for isomer spectroscopy. The target position is in the center of the 15 neutron detectors on the right, surrounded by the N=31 Si–ball shown on a larger scale at the bottom. At the catcher position 60 cm downstream from the target only one Ge-cluster detector is shown. The device on the left side is used for automatic exchange and disposal of the catcher foils to avoid excessive background radiation from radioactivity.

neutrons and charged particles. In Fig. 2 the NORDBALL ancillary detectors are combined with two EUROBALL cluster detectors [13] in close geometry yielding 5 % photo peak efficiency, in a setup designed for isomer spectroscopy. The recoiling residues are stopped on a catcher foil between the cluster detectors 60 cm downstream from the target, which is surrounded by neutron detectors [14] and a charged particle array [15]. The sensitivity of this array, which has been used for the spectroscopy of ^{98}Cd [5] and ^{102}Sn [16] , is estimated to be 10^{-5}. In Fig. 3 the sensitivity limits reached in prompt spectroscopy with the NORDBALL array and ancillary detectors, as described in ref. [2], in the ^{58}Ni+^{50}Cr reaction at 261 MeV are shown in % of the total intensity. Identification of new nuclei with this last generation γ–array was possible on the 10^{-4} level (^{99}Cd), corresponding to a cross section of 25 μb or a production rate of 4 atoms/s at 1 pnA beam and a 2 mg/cm^2 effective target thickness. Similar setups are described in previous papers [2, 11, 12]. Further improvement down to the 10^{-6} level is expected with the 3π of EUROBALL composite Ge–detector part of clover and cluster detectors, implemented by a 1π neutron detector at forward angles and an inner 4π Si–ball, as shown in Fig. 4. The single shell self supporting structure of Si–detectors EUROSiB [17] exploits the pulse shape discrimination technique [18] for charged particle identification in a large dynamic range with low thresholds. Due to its low weight of only 200 g little interference with γ–ray detection is expected. Further details on the cleaning power of ancillary detectors and exit channel identification are given in previous papers and reviews [2, 11, 12].

3 Proton(π)–neutron(ν) interaction at N$\simeq$Z

In Fig. 5 the two–body matrix elements (TBME) for the $(1g_{9/2})^2_{IT}$ multiplet are shown, which were fitted to experimental level schemes close to stability above and close to ^{88}Sr [19]. Besides the I=0, T=1 pairing interaction two strongly bound TBME are found for I=1, 9, T=0, giving rise to proton–neutron pairing at N$\simeq$Z, when protons and neutrons in identical orbits have maximum spatial overlap. As the $\pi\nu$ pairs carry angular momentum, $\pi\nu$ pairing is predicted to dominate at high spin, when I=0,T=1 pairs are reduced due to Coriolis alignment [20]. We have studied in the spherical ($p_{1/2}$, $g_{9/2}$) model space the question of an increasing $\pi\nu$ interaction towards N=Z. In Fig. 6 the decay scheme of the $I^\pi=(14^+)$ spin gap isomer in the T_z=1 nucleus ^{94}Pd is shown, as studied recently with a setup similar to the one shown in Fig. 2 [5]. A shell model calculation in the ($p_{1/2}$, $g_{9/2}$) model space using the empirical interaction of Gross and Frenkel [19] accounts very well for the experimental level scheme, except for the 14^+ - 12^+ spacing ΔE, which experimentally was determined to $\Delta E \leq 80$ keV, as compared to the theoretical ΔE=145 keV. It was found that ΔE is determined entirely by the stretched I=9, T=0 $\pi\nu$ TBME. The experimental limit is reproduced for a 20 % increase of this TBME, indicating an enhanced $\pi\nu$ interaction towards N=Z. This also accounts for the $21/2^+$ - $17/2^+$ level inversion in ^{95}Pd

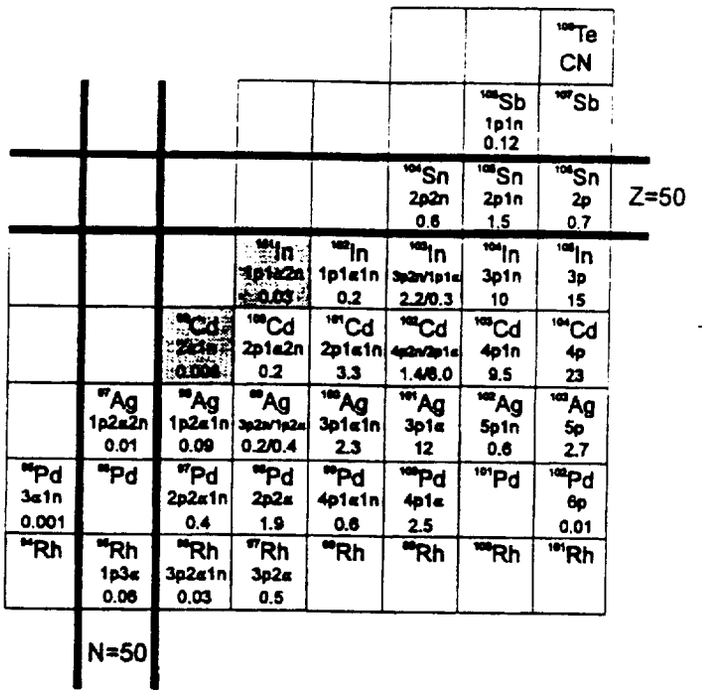

Fig. 3. Detection limits in % of the total residue yield with the NORDBALL array and ancillary detectors for neutrons and charged particles in the reaction ^{58}Ni+^{50}Cr at 261 MeV.

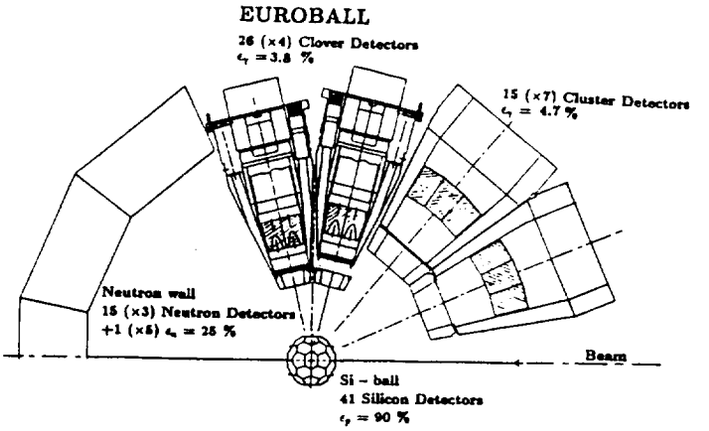

Fig. 4. Schematic view of EUROBALL implemented with ancillary detectors for neutrons and charged particles.

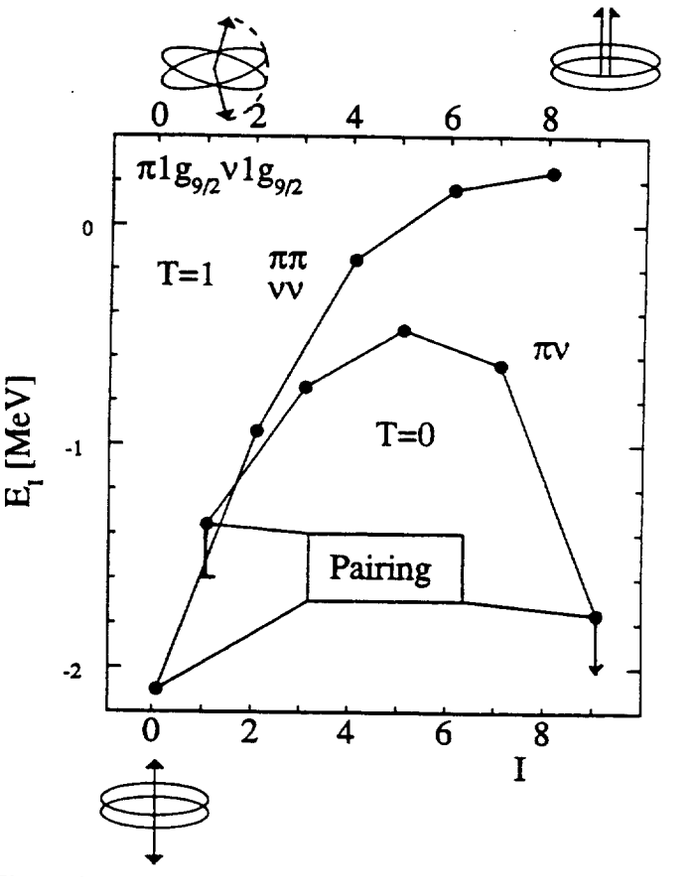

Fig. 5. Interaction energies in the $g^2_{9/2}$ multiplet [19]. Note the strongly bound I=0, 1, 9 states.

[21], causing the spin gap isomerism, which the original interaction of ref. [19] fails to reproduce by a few keV [22]. As for the I=1, T=0 $\pi\nu$ pairing TBME it was found, that it determines indeed the yrast line above the $I^\pi=8^+$ state, where the seniority scheme breaks down due to $\pi\nu$ interaction. In Fig. 7 the spherical yrast lines for the N=48 isotones are compared to shell model calculations. Clearly from ^{92}Ru to ^{96}Cd the development of spin gap isomerism is demonstrated with a predicted ΔI=4 isomer in ^{96}Cd. Also the breakdown of the seniority classification is exhibited by the disappearance of the $I^\pi=8^+$ isomer from ^{92}Ru to ^{94}Pd. Finally, the upper yrast line in ^{92}Ru, the nucleus where the highest spins are reached experimentally [23], can be reproduced best, with an increase of again 20 % of the I=1, T=0 $\pi\nu$ pairing TBME. This first evidence for an increased proton-neutron interaction towards N=Z (see Fig. 5), needs further corroboration in the high spin spectroscopy of ^{92,94}Pd.

Further details of the shell model calculations in this section for the ($p_{1/2}$, $g_{9/2}$) model space are given in previous publications [2, 24].

4 Shell structure of ^{100}Sn and low-lying E2 particle–hole excitations

The experimental spectroscopic data on nuclei close to ^{100}Sn with $T_z \geq 1$ have been analyzed within the spherical shell model. Below ^{100}Sn the restricted ($p_{1/2}$, $g_{9/2}$) configuration space was used for protons and neutrons, whereas above Z=N=50 the full ($d_{5/2}$, $g_{7/2}$, $s_{1/2}$, $d_{3/2}$, $h_{11/2}$) space was allowed. Details of the calculations are described elsewhere [2, 12, 24]. The single particle structure of ^{100}Sn as deduced from the shell model analysis is shown in Fig. 8 in comparison to ^{16}O, ^{40}Ca and ^{56}Ni. With ^{56}Ni the LS closed shells of the light doubly magic N=Z nuclei ^{16}O and ^{40}Ca, change to jj shell closure. This enables strong E2 ph excitations as e.g. $f_{7/2} \rightarrow p_{3/2}$ for ^{56}Ni, both for protons and neutrons, which are stabilized by proton-neutron interaction. The consequences are a strong B(E2;$2^+ \rightarrow 0^+$) in the doubly magic nucleus, as observed in ^{56}Ni [25] , and possibly enhanced effective

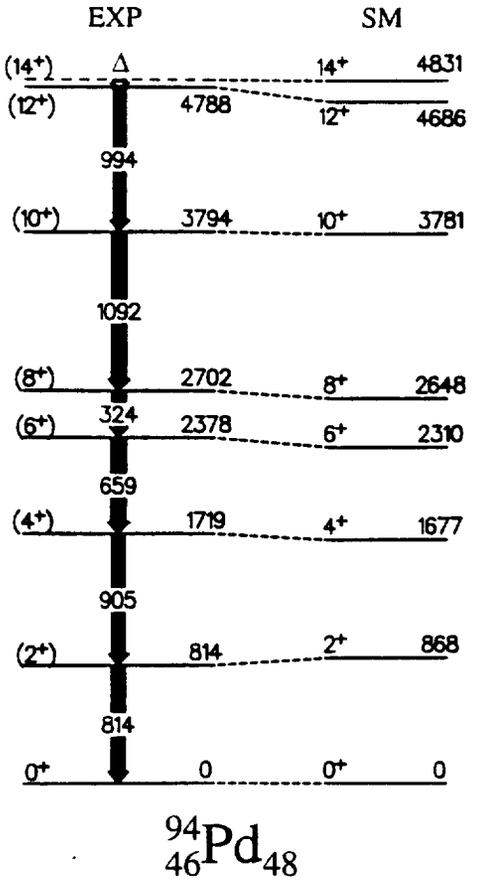

Fig. 6. Experimental and shell model level schemes for ^{94}Pd.

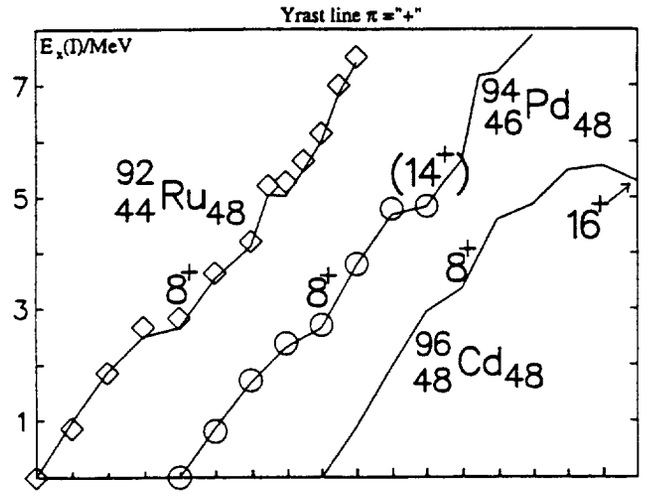

Fig. 7. Experimental and shell model yrast lines for N=48 isotones.

E2 charges.

From the similarity in the shell structure of ^{56}Ni and ^{100}Sn, being separated by one major shell, one would conclude similar expectations for ^{100}Sn. In Table 1 experimental E2 transition strengths from isomers around ^{100}Sn are compared to shell model predictions, obtained with effective charges e_π=1.76 and e_ν=1.44 for protons

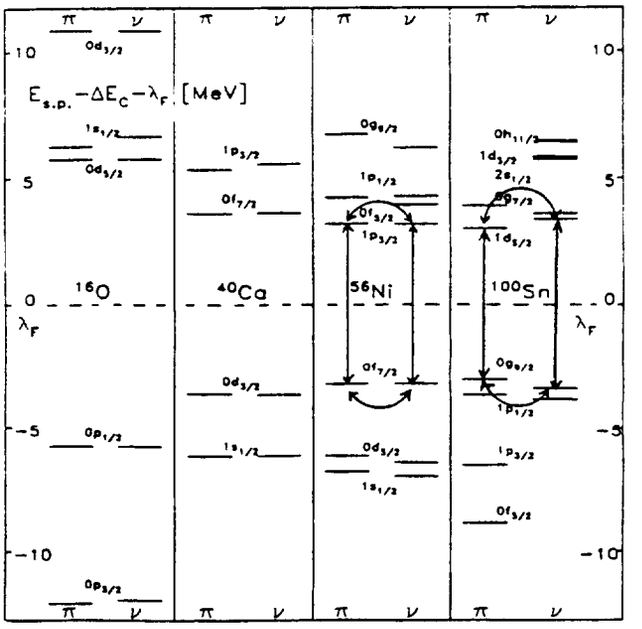

Fig. 8. Single particle (hole) energies for the N=Z doubly magic nuclei ^{16}O, ^{40}Ca, ^{56}Ni, ^{100}Sn, corrected for Coulomb shift ΔE_C and normalized to the middle of the shell gap λ_F.

Table 1. B(E2) strengths in W.u. close to ^{100}Sn

nucleus	$I_i^\pi \rightarrow I_f^\pi$		EX	SM	ref.
^{99}Cd	$17/2^+ \rightarrow 13/2^+$	π	2.5(10)	3.21	[9]
^{101}Cd	$19/2^+ \rightarrow 15/2^+$	π	0.16(1)	0.11	[26]
^{100}Cd	$8^+ \rightarrow 6_2^+$	π	2.6(9)	3.12	[27]
^{100}Cd	$8^+ \rightarrow 6_1^+$	π/ν	0.015(3)	0.003	[27]
^{104}Sn	$6^+ \rightarrow 4^+$	ν	4.0(6)	0.70	[12]
^{106}Sn	$10^+ \rightarrow 8^+$	ν	6.4(10)	3.30	[28]

and neutrons, respectively, as deduced from the ^{88}Sr – ^{90}Zr region [12]. The proton and/or neutron character of the transition is given, too. Obviously, neutron transitions need a much larger effective charge than proton transitions, which are well reproduced by the present choice. This is at variance with RPA predictions for effective charges around ^{100}Sn, yielding $\Delta e_\pi \simeq 1$ and $\Delta e_\nu \simeq 0.7$ for the additional charges [29].

As the experimental evidence on a possible enhancement of the effective charge for protons and neutrons is contradictory and, moreover, as the impurity of the wave functions might mask the results, the obvious next step is the measurement of the respective B(E2) values in the two–proton hole nucleus ^{98}Cd and in the two–neutron nucleus ^{102}Sn. The experiments were performed with the NORDBALL–PEX array shown in Fig. 2. First results for ^{98}Cd are presented in Fig. 9. The level scheme fits perfectly into the systematics of the lighter N=50 isotones ^{92}Mo to ^{96}Pd, the preliminary halflife value of $T_{1/2} \simeq 300$ ns, however, is much longer than expected from the two–proton particle nucleus ^{92}Mo. This cor-

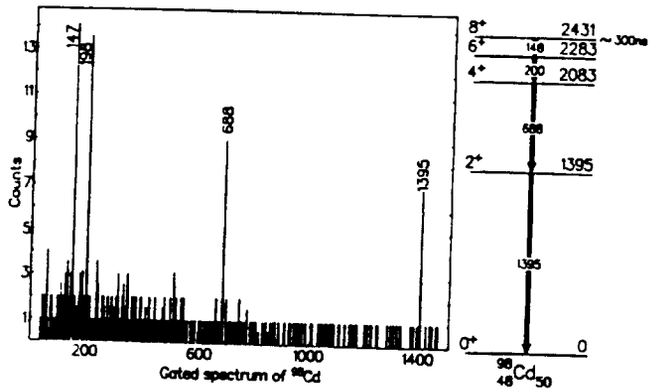

Fig. 9. $\alpha n\gamma\gamma$ coincidence spectrum and level scheme of ^{98}Cd .

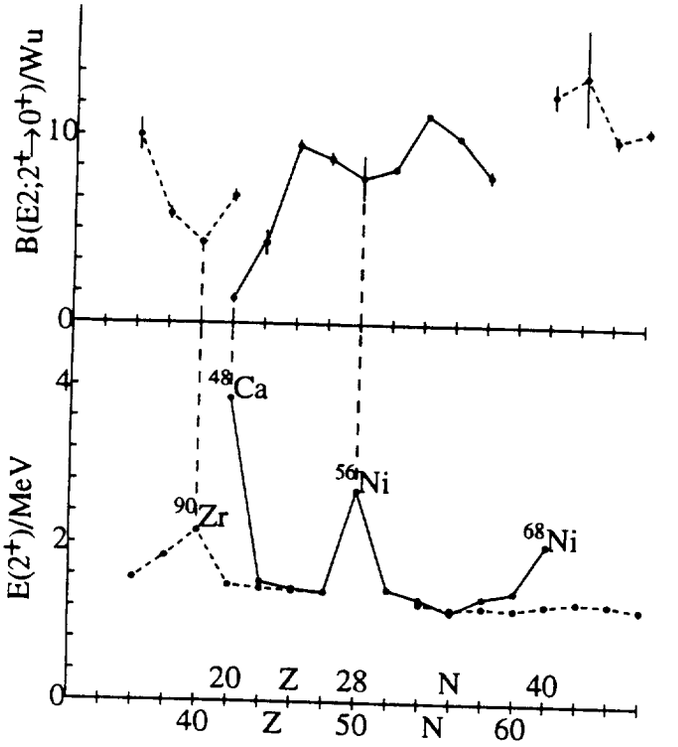

Fig. 10. Systematics of 2^+ excitation energies and $B(E2;2^+\rightarrow 0^+)$ in Ni isotopes and N=28 isotones (full lines) in comparison to Sn isotopes and N=50 isotones (dashed lines).

responds to an effective E2 proton charge of $e_\pi \simeq 1$ in contrast to $e_\pi = 1.76$, reproducing the B(E2) values in the lighter N=50 isotones very well, and also at variance with theory [29]. The final results will be discussed and compared to advanced shell model calculations in a forthcoming paper [6].

The striking similarity in shell structure between ^{56}Ni and ^{100}Sn is nicely exhibited in the systematics of 2^+ excitation energies and $B(E2;2^+\rightarrow 0^+)$ values, shown in Fig. 10. In the close vicinity to the doubly magic nucleus the 2^+ energies seem to be identical both for the proton hole and neutron particle case. This is the more surprising as the nuclear interaction is known to scale with A^{-n} with $1/3 \leq n \leq 1$, depending on whether only surface nucleons or also the bulk of the nucleus participate in the residual interaction. An scaling with A^{-n} would at least result in a 20 % difference of the 2^+ energies, which is not seen in experiment.

5 Future experiments

- The $B(E2;2^+\rightarrow 0^+)$ values in light Sn isotopes and heavy N=50 isotones, measured in relativistic Coulomb excitation of radioactive beams following fragmentation, and the spectroscopy of particle–hole excitations in the now identified ^{98}Cd and ^{102}Sn with the next generation arrays like EUROBALL with ancillary detectors will give information on the role of unbound proton levels, the E2 response of ^{100}Sn and the striking similarity to ^{56}Ni.
- Below ^{100}Sn the proton–neutron pairing can be studied in the high spin spectroscopy of the light Pd and Ru isotopes, which are also predicted to be superdeformed. The steepness of the spherical yrast line in the vicinity of the N=Z=50 shell closure and the proton dripline, may enable proton decay out of superdeformed states.
- Proton and α decay from excited states, even in competition to γ–decay might occur in the lightest Sb and Te isotopes, providing access to the Z>50 shell model space, which is unbound in ^{100}Sn.

References

1. Rykaczewski, K. et al., Inst. Phys. Conf. Ser. No.132: Sect.5, p.517 (1993)
2. Grawe, H. et al., Physica Scripta T56, 71 (1995)
3. Schneider, R. et al., Z. Physik A348, 241 (1994)
4. Lewitowicz, M. et al., Phys. Lett. B332, 20 (1994)
5. Gorska, M. et al., Z. Phys. A 353, 233 (1995)
6. Gorska, M. et al., to be published
7. Arnell, S.E. et al., Phys. Rev. C49, 51 (1994)
8. Alber, D. et al., Z. Phys. A335, 265(1990)
9. Lipoglavsek, M. et al., Phys. Rev. Lett. 76, 888 (1996)
10. Cederkäll, J. et al., Phys. Rev. C53, 1955 (1996)
11. Grawe, H. et al., Acta Physica Polonica B26, 341 (1995)
12. Schubart, R. et al., Z. Phys. A352, 373 (1995)
13. Eberth, J., Proc. Conf. on Physics from Large γ–ray Detector Arrays, August 2-6, 1994, Berkeley, Ca., USA, vol. II, LBL-35687, p.160
14. Arnell, S.E. et al., Nucl. Instr. Meth. A360, 584 (1995)
15. Kuroyanagi, T. et al., Nucl. Instr. Meth. A316, 289 (1992)
16. Lipoglavsek, M. et al., to be published
17. Pausch, G. et al., EUROSiB - A 4π Silicon Ball for Charged Particle Detection in EUROBALL, Project Description, FZ Rossendorf, Germany, 1996
18. Pausch, G. et al., Nucl. Instr. Meth. A365, 176 (1995)
19. Gross, R. and Frenkel, A., Nucl. Phys. A267, 85 (1976)
20. Nazarewicz, W. et al., Physica Scripta T56, 9 (1995)
21. Nolte, E. et al., Z. Phys. A298, 191 (1980)
22. Ogawa, K., Phys. Rev. C28, 958 (1983)
23. Arnell, S.E. et al., Z. Phys. A346, 111 (1993)
24. Rudolph, D., Lieb, K.P., Grawe, H., Nucl. Phys. A597, 298 (1996)
25. Kraus, G. et al., Phys. Rev. Lett. 73, 1773 (1994)
26. Alber, D. et al., Z. Physik A344, 1 (1992)
27. Gorska, M. et al., Z. Physik A350, 181 (1994)
28. Ishii, M. et al. Physica Scripta T56, 89 (1995)
29. Hammamoto, I., private communication